Research Square

Preprints are preliminary reports that have not undergone peer review.
They should not be considered conclusive, used to inform clinical practice,
or referenced by the media as validated information.

Novel Clinical Predictive Model for Stent Dysfunction after TIPS in Patients with Cirrhosis-Related Portal Hypertension

Lei Qin
China Three Gorges University
Qing-Ao Xiao
Central South University
Jing Yu
China Three Gorges University
Wei Li
Jingchu University of Technology
Ji-Dong Yang
Jingchu University of Technology
Wen-Ze Wu
Yangtze University
Mao-Lin Wan
Yangtze University
Xiao-Long Li
China Three Gorges University
Wan-Yao Zhang
China Three Gorges University
Jin-Ke Huang
China Three Gorges University
Xiao-Lin Zhang
zhangxiaolin5800@163.com
China Three Gorges University
Hai-Tao Li
China Three Gorges University

Research Article

Keywords: Transjugular intrahepatic portosystemic shunt, Stent dysfunction, Clinical predictive model, Nomogram

Posted Date: February 3rd, 2026

DOI: https://doi.org/10.21203/rs.3.rs-8531405/v1

License: This work is licensed under a Creative Commons Attribution 4.0 International License.
Read Full License

Additional Declarations: No competing interests reported.

Abstract

Objectives

Transjugular intrahepatic portosystemic shunt (TIPS) is frequently compromised by stent dysfunction (SD). This multi-center retrospective study aimed to develop and validate a predictive tool for post-TIPS SD.

Methods

Between January 2019 and June 2024, 290 TIPS patients from three Chinese hospitals were collected, with 202 eligible cases randomly divided into a training set (n = 141) and an internal validation set (n = 61) at a 7:3 ratio using R software (version 4.2.3). Variable selection was performed via Least Absolute Shrinkage and Selection Operator (LASSO) regression, followed by multivariate logistic regression modeling. Model performance was assessed using the Hosmer-Lemeshow (H-L) test, calibration curves, receiver operating characteristic (ROC) curves, net reclassification improvement (NRI), integrated discrimination improvement (IDI), and decision curve analysis (DCA).

Results

Seven independent predictors of SD were identified: cirrhosis etiology, serum albumin, prothrombin time, blood ammonia, initial stent position, portal vein thrombosis, and maximum transverse diameter of the right hepatic lobe (MTDORHL). The area under the ROC curve (AUC) values of Model C (clinical features), Model R (radiological features), and Model CR (combined features) were 0.823, 0.790, and 0.901 in the training set, and 0.785, 0.736, and 0.866 in the validation set, respectively.

Conclusion

Three SD-specific models were constructed with multi-center data, and Model CR emerged as the optimal one with excellent predictive efficiency and application value, supported by a corresponding nomogram. The identified seven factors serve as independent risk predictors for post-TIPS SD.

Introduction

Portal hypertension represents a major complication of liver cirrhosis, stemming from elevated intrahepatic vascular resistance and increased portal venous pressure. A diagnosis is typically made when the hepatic venous pressure gradient exceeds 5 mmHg, with clinical manifestations becoming apparent beyond 10 mmHg[1,2]. Management of cirrhotic portal hypertension involves various strategies. For acute variceal bleeding (AVB), transjugular intrahepatic portosystemic shunt (TIPS) placement achieves high technical success rates of 93%-100% and its effect on refractory ascites related to portal

hypertension is relatively variable, with reported efficacy ranging from 50% to 90%[3,4]. A significant factor limiting the long-term benefit of TIPS is stent dysfunction (SD), primarily caused by stent stenosis or occlusion[5]. SD leads to shunt failure, recurrence of portal hypertension, and complications such as variceal rebleeding or ascites, adversely affecting patient quality of life and long-term survival[6]. The pathogenesis of SD is multifactorial, involving processes like pseudointimal hyperplasia (often associated with bile leakage), acute thrombosis, and the formation of a "stent cap"[7–10]. Reported incidence rates vary widely, from 14% to 82% within the first year post-TIPS[11]. Despite advances like PTFE-covered stents and routine postoperative anticoagulation[12], stent patency issues still occur in 8%-20% of patients[13]. This has a huge impact on clinical practice. For instance, one study noted SD in all patients experiencing ascites or rebleeding within 30 days of TIPS[14]. Current predictive models for SD often focus narrowly on specific patient groups, such as those with hepatitis B-related cirrhosis, and suffer from limitations like single-center design and restrictive inclusion criteria[15]. This limits their generalizability. Our study addresses this gap by utilizing a multi-center cohort that includes patients with diverse etiologies of cirrhosis.

We aimed to develop and validate a more broadly applicable predictive tool for post-TIPS SD, which would assist in risk stratification and guide personalized patient management to improve long-term shunt patency.

Ethics statement

This study was granted ethical clearance by the Ethics Committee of the First College of Clinical Medical Science, China Three Gorges University (Approval No. 2024-232-01), in compliance with relevant ethical guidelines. Consistent with local regulatory requirements and institutional procedures, written informed consent was exempted for this retrospective investigation.

Consent to participate

Given the retrospective nature of this study, which involved the analysis of anonymized clinical data, the requirement for written informed consent was waived by the Ethics Committee of the First College of Clinical Medical Science, China Three Gorges University

Materials and Methods

Study design

This multi-center retrospective investigation enrolled patients with cirrhotic portal hypertension who underwent TIPS across three medical centers in China from January 2019 to June 2024. The specific flowchart of this study is presented in Figure 1. Inclusion in the cohort was restricted to patients who met all four of the below-stated criteria: (1) Age ≥ 18 years; (2) Patients with acute esophagogastric variceal bleeding who were ineffective after endoscopic conservative treatment; (3) Refractory ascites

caused by cirrhotic portal hypertension; (4) Regular review or telephone follow-up for at least 1 year. Exclusion criteria: (1) Surgical failure; (2) Serious systemic disease; (3) Extensive missing clinical data; (4) Follow-up duration < 1 year or loss to follow-up beyond 1 year.

Data collection and Follow-up

Relevant clinical information was systematically gathered and analyzed for the present study: gender (male/female), age, cirrhosis etiology of cirrhosis (hepatitis B, hepatitis C, alcoholic cirrhosis, cholestatic cirrhosis, schistosomiasis, autoimmune cirrhosis, Wilson's disease, idiopathic portal hypertension), postoperative anticoagulation (Yes/no), splenectomy (Yes/No), portal vein thrombosis (PVT, Yes/No), portal cavernoma (Yes/No), diabetes mellitus (Yes/No), hypertension (Yes/No), complete blood count, sodium, potassium, calcium, ammonia, international normalized ratio (INR), prothrombin time (PT), prothrombin activity (PTA), activated partial thromboplastin time (APTT), thrombin time (TT), serum creatinine, total bilirubin, indirect bilirubin, alanine aminotransferase (ALT), aspartate aminotransferase (AST), albumin, Child-Pugh score and classification, diameter of the portal vein, diameter of the splenic vein, type of shunt (esophagogastric, splenorenal, gastrorenal) , maximum diameter of both liver lobes, portal vein shunt branches (right, left, main trunk), stent diameter, stent type (bare metal stent, single covered stent, combo of bare metal and covered stents), initial stent position (optimal, suboptimal)[11,16] (1) the proximal end of the stent extends to the hepatic venous junction; (2) the distal end of the stent is parallel to the wall of the portal vein (the angle between the tangential line of the distal end and the portal vein wall is less than 20°). Otherwise, the stent position is defined as suboptimal. The follow-up period is one year, with the primary endpoint being stent dysfunction.

The researchers reviewed the patient 's admission records in detail. If the patient is not followed up regularly within 1 year, the patient will be contacted by telephone to determine whether the patient is examined in other institutions and the stent status after examination. If the patient's follow-up data is lost, the patient is excluded.

Stent dysfunction assessment

The patient 's clinical manifestations or imaging examination suggested that the stent function may be impaired[16-18]: (1) Recurrence of complications associated with portal hypertension; (2) Portal vein color Doppler ultrasound showing blood flow velocity within the stent > 250 cm/s or < 50 cm/s; (3) Hepatic enhanced CT indicating stenosis or occlusion of the stent lumen. The final criterion for verifying stent patency was portal venography under DSA.

Risk factor screening

We employed LASSO logistic regression for variable selection due to its built-in ability to handle multicollinearity and reduce overfitting risk [19,20]. During the variable selection procedure, we used two thresholds (λmin and λ1-SE)[21]. The variables with the λmin threshold value were included in the multivariate analysis. Independent risk factors of stent dysfunction were defined as having statistical

significance (two-sided P<0.05). To differentiate between the predictors derived from each type of data, we ran separate screening steps on clinical and radiology variables respectively, which enabled us to train specialized models per class.

Model construction and comparison

We randomly stratified all 202 participants with an overall split of 70% (n=141) for the training set and 30% (n=61) for the testing set using R software We constructed three models aiming at predicting the primary outcome: Model C (clinical features only).Model R (based only on radiological features) , and Model CR (combining both clinical-biochemical and radiological information).After univariate analysis on the training cohort, variables with P < 0.05 were subjected to step-wise selection and then enter in to a multivariate logistic regression, a procedure that was designed to identify independent variables predictive for post-TIPS SD. Predictors were presented According to the identified independent predictors, a nomogram predicting probability of stent dysfunction at 1 year after TIPS was built. Two-sided P-values <0.05 were regarded as statistically significant. Comparative assessments were conducted for the ROC curve, area under the receiver operating characteristic curve (AUC), net reclassification improvement (NRI), integrated discrimination improvement (IDI), and calibration curve. The prediction effect of the above model prediction model is verified by using the verification set data, and the advantages and disadvantages of the best model and the other models are compared after determining the best model. Finally, the decision curve analysis (DCA) were performed in order to evaluate the potential benefit for all models. The baseline demographic and clinic features between the two groups are compared by a t-test or a chi-square test, respectively.

We compared model discrimination with the DeLong test for AUCs; additionally calculated the NRI and IDI to measure the incremental predictive value of the more complicated models. We evaluated calibration by developed calibration curves for visual inspection of agreement between predicted probability and observed outcome, for the training cohort as well as the validation cohort. We used the Hosmer-Lemeshow (H-L) test to evaluate statistical evidence about model calibration, p-value > 0.05 indicating acceptable calibration. Once an ideal model is selected (Model CR), then a nomogram was developed for transforming the independent predictors into personalized risk scores, enabling quantified prediction of the likelihood of post-TIPS SD. We further assessed the clinical utility of the nomogram with DCA, which computed the net benefit for various threshold probabilities and therefore demonstrated how it could be used to inform decisions about patient.

Statistical analysis

The CBCgrp (Version1.0.1) package within R software (Version 4.2.3) was used to carry out statistical analyses, encompassing the description of baseline characteristics and specificity analysis. Continuous data were summarized as mean ± standard deviation or median with interquartile range, while categorical data were expressed as counts and percentages[22]. Intergroup comparisons of continuous variables were performed using independent samples t-tests or Wilcoxon rank-sum tests (non-normal

distribution), and categorical variables were compared using Pearson's chi-square tests or Fisher's exact tests. P-value < 0.05 was considered statistically significant.

Results

Patient characteristics

In this study, a total of 290 patients with TIPS were collected, and 88 patients who did not meet the requirements were excluded. For some missing data variables, the missing values were multiply imputed by the mice (Version 3.16.0) function, and the variables with a missing amount of more than 20 % were deleted. Finally, 202 patients treated with TIPS were included.

There were 31 patients (15%) with stent dysfunction. Baseline tables were drawn according to the training set and validation set, and whether stent dysfunction occurred (Table 1).

Risk factors for dysfunction

LASSO regression was used to take non-zero coefficient variables at λmin (Figure 2). After LASSO regression analysis of clinical factors, five variables (λmin = 0.034, λ1-SE = 0.078) were screened out: cirrhosis etiology, total bilirubin, albumin, prothrombin time and blood ammonia (Figure 2A); four variables (λmin = 0.021, λ1-SE = 0.083) were screened out by imaging factors, including stent type, maximum transverse diameter of right lobe of liver, initial stent position and portal vein embolus (Figure 2B).

After finalizing the candidate variables, multivariate logistic regression was utilized to perform statistical analysis on these selected factors (Table 2, Table 3). The final independent risk factors for postoperative SD included the cirrhosis etiology (OR : 0.613,95% CI : 0.413-0.908), albumin (OR : 0.87,95% CI : 0.776-0.974), prothrombin time (OR : 0.668,95% CI : 0.481-0.926), blood ammonia (OR : 1.009,95% CI : 1.001-1.017), initial stent position (OR : 0.25,95% CI : 0.069-0.906), maximum transverse diameter of right hepatic lobe (OR : 1.366,95% CI : 1.073-1.738) and portal vein emboli (OR : 2.159,95%CI :1.021-4.564).

Model comparison

The discrimination capacity of Model CR was superior among those patients who were part of the training cohort [AUC = 0.901(95%CI:0.839-0.962)] than both models, Model C (AUC = 0.823), Model R(AUC=0.790). The same hierarchy of performance between these three models (Model CR > Model C > Model R) was repeated in the validation cohort, demonstrating that predictions from this combined model were reliable. The diagnostic performance of each model, including sensitivity, specificity, the optimal threshold (Youden index), and AUC, is presented in Table 4. In order to find out if the difference of AUC was significant or not, we used the DeLong test (Table 5). Although there was a significant difference between Model R and Model CR in the training set (P=0.029), was not so for the validation set (P = 0.062). In fact, there were no statistically significant differences in AUC among the three models in the validation set. We further calculated the NRI and IDI based on training set and found that compared

to Model C and R respectively, Model CR had a statistical significance higher performance. The same phenomenon existed partly in validation set, where Model CR showed significantly better NRI than the other two models but no significant difference in NRI between Model C and Model R themselves ($P > 0.05$).

Model fit was assessed using calibration curves (Figure 4) and the H-L test. All three models demonstrated good calibration, with good agreement to what was observed clinically (Figure 4and Table 6). Collectively, these comparisons demonstrated that Model CR provided the best and most consistent predictions across both the training set and the validation set. Thus, the best-performing model (CR) is selected to use in all of our following analysis.

Model visualization

Furthermore, we constructed nomogram of best Model CR (Figure 5) based on the screening results of risk factors by LASSO regression and verified by multivariable logistic regression. The individual risk score of each patient was calculated according to the total score obtained from all independent predictors in the nomogram, which allows quantitatively estimate post-TIPS SD risk. Besides, DCA curve was also generated in order to calculate the patient's potential benefit following TIPS. The result shows that Model CR's net benefit range is bigger compared to the other two models, and this conclusion can be drawn on both training set and validation set. (Figure 6)

Discussion

As one of the most serious complications after TIPS, SD has significant negative effects on long term survival rate and prognosis of patients with TIPS. In order to accurately predict the occurrence rate of SD after TIPS, the relevant risk factors need to be identified. Currently, the risk of SD remains elusive. Existing prediction models on post-TIPS shunt failure were limited to a subset of cirrhosis types, mainly for liver disease caused by hepatitis b. These-subtype specific instruments are not sufficient for capturing the complexity in differentiating cirrhotics on account of the interaction between various etiology, clinical and radiologic features that we seek to do so through this investigation using data from several centers including several causes of liver disease as well as merging clinical/biochemical variables with radiologic measurements.

In addition, by incorporating the imaging variables into the clinical information in our multi-center cohort, we developed an integrative model (Model CR), and this joint model also achieved good prediction results, with an AUC of 0.901 (sensitivity 73.7% and specificity 89.3%) on the training set. It also performed well on the validation set with an AUC of 0.866 (sensitivity 66.7%, specificity 87.8%). Previous studies have associated the occurrence of SD with several factors such as splenectomy, diabetes, portosystemic shunt type, portal vein diameter, PVT, and the initial stent position[15,22-24]. SD generally occurs in one of two time frames: early (within one week), which is usually caused by an acute thrombosis, while late failure is commonly due to pseudointimal hyperplasia or hepatic vein stenosis[8].

The independent clinical risk factors for SD that we found were as follows: cirrhosis etiology, serum albumin level, PT, blood ammonia level, initial stent position, PVT, and MTDORHL.

In line with the nation's epidemiology, cirrhotic liver disease due to viral hepatitis was the most common etiology among our cohort, followed by alcoholic cirrhosis. Interestingly, cirrhosis etiology was also found to be an independent predictor for SD. It might have been due to different pathophysiological backgrounds among different causes. Chronic neutrophilic inflammation and accumulation are frequently observed in alcoholic cirrhosis, Kupffer cells activation and increased pro-inflammatory cytokines that may favor the endothelium injury and thrombosis. On the other hand, the inflammatory activity in viral hepatitis can often be controlled with long-term antiviral therapy, thus possibly eliminating at least some of the SD risk factors[25]. Hypoalbuminaemia has several ways of contributing to SD, including being linked to a more sluggish portal flow (which favours thrombosis)impaired endothelial repair, and immunodeficiency which could predispose patients to stent related inflammation and infection[26,27], which in combination create a prothrombotic/intimal-fibrotic milieu that accelerates stent occlusion. We found PT independently predictive too. Despite the fact that the PT is usually prolonged by cirrhosis, we found a paradoxically shortened PT in some of our patients – 18%, specifically among PVT cases. We consider this indicative of a hypercoagulable state, which is associated with increased risk of acute stent thrombosis[28].

High ammonia levels seem to increase SD risk in our model. In decompensated cirrhosis, liver cell dysfunction leads to urea-cycle disruption and leading to hyperammonemia[29]. The median ammonia value in our cohort was 57.5 μmol/L, but it still turned out to be an independent factor for SD on multivariate analysis (OR: 1.009) although there is no evidence that ammonia has any relation with stent occlusion so far, new data suggest that ammonia may modulate the inflammatory pathways. We hypothesize that in our patients increased ammonia might have triggered pro-inflammatory cytokines such as TNF-a or IL-6, which then might trigger coagulation and a local pro-thrombotic environment inside the stent[30].

Initial stent position was confirmed as an independent predictor of SD in our analysis, supporting earlier reports in the literature[15]. We could further define this relationship with technical parameters of what constitutes poor stent positioning (failure to traverse into the hepatocaval junction, angulation >20° from portal vein wall) where such stents had 3.8 times the risk of developing dysfunction. Mechanistically , if a stent fails to reach the hepatic vein confluence, then there is a niche for turbulent flow and endothelial injury. promoting pseudointimal hyperplasia, which in turn serves as a nidus for hepatic vein stenosis/thrombus formation, driving stent failure[11,31-34]. Inappropriate stent positioning (i.e., a hepatic vein stent positioned too inferiorly or a portal vein stent that is not long enough),which predisposes to the formation of a "stent cap", which alters normal hemodynamics, eventually resulting in stent failure[22]. Moreover, Clark et al. reported that TIPS extension to the hepatocaval junction confers a longer shunt longevity when compared with stents terminated in the hepatic vein, which agrees with our observation

of structural insufficiency (e.g., short stent length, high tangential angle) disrupting the hemodynamic environment and promoting pseudo-intimal hyperplasia or thrombus formation[32].

Additionally, portal vein embolus is also one of its important risk factors. According to different sources, it is divided into thrombus and tumor thrombus, among which thrombus accounts for a higher proportion. PVT is not a contraindication for TIPS at present. By establishing portosystemic shunt and postoperative anticoagulation, the patency rate after stenting is usually not affected. However, in a small proportion of clinical cases, PVT that involves the superior mesenteric vein or lienal vein not only affects the operability of stent placement but also augments the risk of postoperative functional complications, which originate from the patients' substantial thrombus load and inherent hypercoagulability[24]. The risk profile is significantly worse in those presenting with portal vein tumour thrombus; in this patient population, stent occlusion risk is increased by the tumour's invasive and crushing nature as well as the profound hemodynamic changes of progressive cancer[35,36].

We demonstrate that the value of liver morphology, identifying the maximum transverse diameter of the right hepatic lobe (MTDORHL) as an innovative, independent risk factor for SD (OR: 1.366). The median MTDORHL in our cohort is 9.57cm, while compensatory right lobe hypertrophy existed in 38.6% of the patients. Enlargement may mechanically compress the adjacent right portal vein branch and right hepatic vein, thus contributing to increase in local vascular resistance. This resulting haemodynamic abnormality favours a pro-thrombotic environment as well as intimal proliferation inside the stent, furthermore, the swollen liver tissue itself can exert physical pressure on the stent with time and change its trajectory or cause mechanical occlusionn[37,38].

We therefore developed a clinical nomogram based on Model CR's independent predictors. This graphical tool enables physicians to quickly estimate a patient's risk of stent dysfunction at a glance, facilitating risk-stratified clinical management after TIPS.

While promising, our model's limitations must be acknowledged. The study is retrospective, with limited sample sizes for some cirrhosis etiologies and without confirmatory venography in all suspected SD cases, potentially introducing bias. Image measurement by hand can be a source of variation as well. Therefore, the next important step will be external validation using prospective, larger scale experiments. This will aid in improving the predictive capacity of this model, bringing it one step closer to being used as an all-inclusive clinical tool for managing patients with TIPS.

Conclusions

According to our multi-center retrospective cohort, we built three prediction models of post-TIPS stent dysfunction and Model CR (the combined clinical-radiological model) performed best, which demonstrated best and most clinically informative prediction results, enabling individualized treatment through precise patient risk stratification, thus influencing both the level of monitoring and the time at which an intervention may be required.

Declarations

Availability of data and materials

The datasets used or analyzed during the current study are available from the corresponding author on reasonable request. All data are stored in a secure server at the First College of Clinical Medical Science, China Three Gorges University.

Authors contribution

Lei Qin, Qing-Ao Xiao: Data collection, Statistical analysis, Writing - original draft; Jing Yu, Wei Li, Wen-Ze Wu: Data collection, Statistical analysis; Ji-Dong Yang, Mao-Lin Wan, Xiao-Long Li, Wan-Yao Zhang, Jin-Ke Huang: Data collection; Xiao-Lin Zhang, Hai-Tao Li: Writing – review & editing (equal corresponding contribution).

Competing interests

The authors declare that they have no competing interests. No funding bodies had any role in the design of the study, collection, analysis, interpretation of data, or writing the manuscript.

FUNDING

No funding was provided for this work.

ACKNOWLEDGMENTS

We would like to sincerely acknowledge and thank the First College of Clinical Medical Science at China Three Gorges University, Jingzhou Central Hospital, and Jingmen People's Hospital for their valuable support in this study.

References

1. Simonetto DA, Liu M, Kamath PS. Apr. Portal Hypertension and Related Complications: Diagnosis and Management. *Mayo Clinic proceedings*. 2019;94(4):714–726. 10.1016/j.mayocp.2018.12.020
2. Baffy G, Bosch J. Overlooked subclinical portal hypertension in non-cirrhotic NAFLD: Is it real and how to measure it? J Hepatol Feb. 2022;76(2):458–63. 10.1016/j.jhep.2021.09.029.
3. Azoulay D, Castaing D, Majno P, et al. Salvage transjugular intrahepatic portosystemic shunt for uncontrolled variceal bleeding in patients with decompensated cirrhosis. J Hepatol Nov. 2001;35(5):590–7. 10.1016/s0168-8278(01)00185-4.
4. Riggio O, Ridola L, Angeloni S, et al. Clinical efficacy of transjugular intrahepatic portosystemic shunt created with covered stents with different diameters: results of a randomized controlled trial. J Hepatol Aug. 2010;53(2):267–72. 10.1016/j.jhep.2010.02.033.

5. Pitton MB, Müller L, Stoehr F, et al. Transjugular intrahepatic portosystemic shunt with ePTFE-covered stentgrafts: incidence and predictors of shunt dysfunction. Insights Imaging Nov. 2025;5(1):244. 10.1186/s13244-025-02122-2.
6. Wan YM, Li YH, Xu Y, et al. Predictors of Shunt Dysfunction and Overall Survival in Patients with Variceal Bleeding Treated with Transjugular Portosystemic Shunt Creation Using the Fluency Stent Graft. Acad Radiol Jul. 2018;25(7):925–34. 10.1016/j.acra.2017.11.020.
7. Saltini D, Indulti F, Guasconi T, et al. Transjugular Intrahepatic Portosystemic Shunt: Devices Evolution, Technical Tips and Future Perspectives. Journal Clin medicine Oct. 2023;25(21). 10.3390/jcm12216758.
8. Büttner L, Pick L, Jonczyk M, et al. Shunt dysfunction and mortality after transjugular intrahepatic portosystemic shunt (TIPS) in patients with portal hypertension. Insights Imaging Aug. 2024;7(1):193. 10.1186/s13244-024-01768-8.
9. Yao X, He S, Wei M, Qin JP. Influence of different portal vein branches on hepatic encephalopathy during intrahepatic portal shunt via jugular vein. World J Gastroenterol Aug. 2022;21(31):4467–70. 10.3748/wjg.v28.i31.4467.
10. Dissegna D, Sponza M, Falleti E, et al. Morbidity and mortality after transjugular intrahepatic portosystemic shunt placement in patients with cirrhosis. Eur J Gastroenterol Hepatol. May 2019;31(5):626–32. 10.1097/meg.0000000000001342.
11. Bai M, He CY, Qi XS, et al. Shunting branch of portal vein and stent position predict survival after transjugular intrahepatic portosystemic shunt. World J Gastroenterol Jan. 2014;21(3):774–85. 10.3748/wjg.v20.i3.774.
12. Gaba RC, Bui JT, Cotler SJ, et al. Rebleeding rates following TIPS for variceal hemorrhage in the Viatorr era: TIPS alone versus TIPS with variceal embolization. Hepatology international Aug. 2010;6(4):749–56. 10.1007/s12072-010-9206-2.
13. Wang X, Zhu Y, Zhu M, Luo X, Yang L. Mar. Combined Y-configured stents for revising occluded transjugular intrahepatic portosystemic shunt. *Diagnostic and interventional radiology (Ankara, Turkey)*. 2021;27(2):238–43. 10.5152/dir.2021.20036
14. Sarwar A, Weinstein JL, Novack V, et al. Causes and Rates of 30-Day Readmissions After Transjugular Intrahepatic Portosystemic Shunts. AJR Am J roentgenology Jul. 2020;215(1):235–41. 10.2214/ajr.19.21732.
15. Zhan P-c, Li Z, Li X, et al. A Nomogram to Predict the Risk of Stent Dysfunction After TIPS in Patients with Hepatitis B Cirrhosis. Acad Radiol. 2022;29(10):1532–40. 10.1016/j.acra.2022.01.016.
16. Mamone G, Milazzo M, Di Piazza A et al. Dec. Transjugular intrahepatic portosystemic shunt (TIPS) complications: what diagnostic radiologists should know. *Abdominal radiology (New York)*. 2022;47(12):4254–4270. 10.1007/s00261-022-03685-0
17. Hayek G, Ronot M, Plessier A, et al. Long-term Outcome and Analysis of Dysfunction of Transjugular Intrahepatic Portosystemic Shunt Placement in Chronic Primary Budd-Chiari Syndrome. Radiology Apr. 2017;283(1):280–92. 10.1148/radiol.2016152641.

18. Huang Z, Yao Q, Zhu J, et al. Efficacy and safety of transjugular intrahepatic portosystemic shunt (TIPS) created using covered stents of different diameters: A systematic review and meta-analysis. Diagn Interv Imaging. 2021;102(5):279–85. 10.1016/j.diii.2020.11.004.
19. Friedman J, Hastie T, Tibshirani R. Regularization Paths for Generalized Linear Models via Coordinate Descent. J Stat Softw. 2010;33(1):1–22.
20. Huang YQ, Liang CH, He L, et al. Development and Validation of a Radiomics Nomogram for Preoperative Prediction of Lymph Node Metastasis in Colorectal Cancer. Journal Clin oncology: official J Am Soc Clin Oncology Jun. 2016;20(18):2157–64. 10.1200/jco.2015.65.9128.
21. Chen X, Zhang H, Guo D, et al. Risk of intraoperative hemorrhage during cesarean scar ectopic pregnancy surgery: development and validation of an interpretable machine learning prediction model. EClinicalMedicine Dec. 2024;78:102969. 10.1016/j.eclinm.2024.102969.
22. Bai Y, Liu J, Wang C, et al. Comparison of specialized stent versus generic stent and bare stent combination for transjugular intrahepatic portosystemic shunt creation. Scientific reports Jun. 2024;23(1):14439. 10.1038/s41598-024-64358-0.
23. Lv Y, Bai W, Li K, et al. Anticoagulation and Transjugular Intrahepatic Portosystemic Shunt for the Management of Portal Vein Thrombosis in Cirrhosis: A Prospective Observational Study. The Am J gastroenterology Jul. 2021;1(7):1447–64. 10.14309/ajg.0000000000001194.
24. Qi X, He C, Guo W, et al. Transjugular intrahepatic portosystemic shunt for portal vein thrombosis with variceal bleeding in liver cirrhosis: outcomes and predictors in a prospective cohort study. Liver international: official J Int Association Study Liver May. 2016;36(5):667–76. 10.1111/liv.12929.
25. Bertoletti A. The immune response in chronic HBV infection. Journal viral hepatitis Dec. 2024;31(Suppl 2):43–55. 10.1111/jvh.13962.
26. Allison SP, Lobo DN. Apr. The clinical significance of hypoalbuminaemia. *Clinical nutrition (Edinburgh, Scotland)*. 2024;43(4):909–14. 10.1016/j.clnu.2024.02.018
27. Valeriani E, Pannunzio A, Palumbo IM, et al. Risk of venous thromboembolism and arterial events in patients with hypoalbuminemia: a comprehensive meta-analysis of more than 2 million patients. Journal Thromb haemostasis: JTH Oct. 2024;22(10):2823–33. 10.1016/j.jtha.2024.06.018.
28. Li X, Wang HL, Zhou TY, et al. [Analysis of influencing factors of shunt dysfunction after transjugular intrahepatic portosystemic shunt in liver cirrhosis accompanied with portal vein thrombosis]. *Zhonghua gan zang bing za zhi = Zhonghua ganzangbing zazhi = Chinese journal of hepatology*. Sep. 2020;20(9):742–6. 10.3760/cma.j.cn501113-20200301-00079.
29. Engelmann C, Clària J, Szabo G, Bosch J, Bernardi M. Pathophysiology of decompensated cirrhosis: Portal hypertension, circulatory dysfunction, inflammation, metabolism and mitochondrial dysfunction. J Hepatol Jul. 2021;75(Suppl 1):S49–66. 10.1016/j.jhep.2021.01.002.
30. Aldridge DR, Tranah EJ, Shawcross DL. Pathogenesis of hepatic encephalopathy: role of ammonia and systemic inflammation. Journal Clin experimental hepatology Mar. 2015;5(Suppl 1):S7–20. 10.1016/j.jceh.2014.06.004.

31. Lee EW, Eghtesad B, Garcia-Tsao G, et al. AASLD Practice Guidance on the use of TIPS, variceal embolization, and retrograde transvenous obliteration in the management of variceal hemorrhage. Hepatology Jan. 2024;1(1):224–50. 10.1097/hep.0000000000000530.
32. Clark TW, Agarwal R, Haskal ZJ, Stavropoulos SW. The effect of initial shunt outflow position on patency of transjugular intrahepatic portosystemic shunts. Journal vascular interventional radiology: JVIR Feb. 2004;15(2 Pt 1):147–52. 10.1097/01.rvi.0000109401.52762.56.
33. Luo X, Nie L, Tsauo J, Wang Z, Tang C, Li X. Parallel shunt for the treatment of transjugular intrahepatic portosystemic shunt dysfunction. Korean J radiology May-Jun. 2013;14(3):423–9. 10.3348/kjr.2013.14.3.423.
34. Sun SH, Eche T, Dorczynski C et al. May. Predicting death or recurrence of portal hypertension symptoms after TIPS procedures. *European radiology*. 2022;32(5):3346–57. 10.1007/s00330-021-08437-0
35. Norero B, Bosch J, Berzigotti A, Rodrigues SG. Transjugular intrahepatic portosystemic shunt in patients with hepatocellular carcinoma: A systematic review. United Eur Gastroenterol journal Oct. 2023;11(8):733–44. 10.1002/ueg2.12454.
36. Giri S, Singh A, Das S, et al. Efficacy and safety of transjugular intrahepatic portosystemic shunt in patients with hepatocellular carcinoma-A systematic review and meta-analysis. Indian J gastroenterology: official J Indian Soc Gastroenterology Dec. 2024;43(6):1121–35. 10.1007/s12664-024-01646-7.
37. Chen SL, Hu P, Lin ZP, Zhao JB. The Effect of Puncture Sites of Portal Vein in TIPS with ePTFE-Covered Stents on Postoperative Long-Term Clinical Efficacy. Gastroenterol Res Pract. 2019;2019:2935498. 10.1155/2019/2935498.
38. Cura M, Cura A, Suri R, El-Merhi F, Lopera J, Kroma G. Causes of TIPS dysfunction. AJR Am J roentgenology Dec. 2008;191(6):1751–7. 10.2214/ajr.07.3534.

Tables

Table1. The baseline characteristics of cirrhosis patients undergoing TIPS

Variables	Total (n = 202)	Training set (n = 141)	Validation set (n = 61)	*P*
Sex, n (%)				0.588
Female	82 (41)	55 (39)	27 (44)	
Male	120 (59)	86 (61)	34 (56)	
Age, Mean ± SD	59.17 ± 9.75	58.38 ± 9.82	60.98 ± 9.42	0.078
Cirrhosis etiology, n (%)				0.730
HBV	90 (45)	67 (48)	23 (38)	
HCV	10 (5)	7 (5)	3 (5)	
Alcohol	54 (27)	35 (25)	19 (31)	
Schistosome	45 (22)	30 (21)	15 (25)	
Other	3 (1)	2 (1)	1 (2)	
Type of shunt channel, n (%)				0.158
Esophageal gastric fundus shunt	188 (93)	134 (95)	54 (89)	
Spleen-kidney collateral shunt	11 (5)	5 (4)	6 (10)	
Gastrorenal shunt	3 (1)	2 (1)	1 (2)	
Shunting branch of the PV, n (%)				0.072
Left	98 (49)	74 (52)	24 (39)	
Right	88 (44)	54 (38)	34 (56)	
Trunk	16 (8)	13 (9)	3 (5)	
Stent diameter (mm), n (%)				0.207
6	25 (12)	21 (15)	4 (7)	
7	24 (12)	17 (12)	7 (11)	
8	149 (74)	99 (70)	50 (82)	
10	4 (2)	4 (3)	0 (0)	
Initial stent position, n (%)				0.818
Superior	120 (59)	85 (60)	35 (57)	
Suboptimal	82 (41)	56 (40)	26 (43)	
Types of stents, n (%)				0.642

Uncovered stents	114 (56)	77 (55)	37 (61)	
Covered stent	6 (3)	4 (3)	2 (3)	
Combination stent	82 (41)	60 (43)	22 (36)	
Preoperative ascites, n (%)				0.898
None	58 (29)	41 (29)	17 (28)	
Less	104 (51)	74 (52)	30 (49)	
Medium	22 (11)	14 (10)	8 (13)	
Mass	18 (9)	12 (9)	6 (10)	
Preoperative anticoagulation, n (%)				0.317
Yes	198 (98)	137 (97)	61 (100)	
No	4 (2)	4 (3)	0 (0)	
Postoperative anticoagulant, n (%)				0.188
Yes	92 (46)	69 (49)	23 (38)	
No	110 (54)	72 (51)	38 (62)	
Splenectomy, n (%)				0.897
Yes	165 (82)	116 (82)	49 (80)	
No	37 (18)	25 (18)	12 (20)	
Diabetes, n (%)				0.992
Yes	38 (19)	26 (18)	12 (20)	
No	164 (81)	115 (82)	49 (80)	
Hypertension, n (%)				0.945
Yes	32 (16)	23 (16)	9 (15)	
No	170 (84)	118 (84)	52 (85)	
Hemoglobin, Median (Q1,Q3)	71.50 (62.25, 86)	71.00 (62, 88)	73.00 (64, 86)	0.950
C reactive protein, Median (Q1,Q3)	3.82 (1.68, 12.61)	3.9 (1.63, 14.66)	3.77 (1.92, 8.06)	0.463
Glutamic pyruvic transaminase, Median (Q1,Q3)	20 (14, 27)	20 (14, 26)	20 (15, 30)	0.382
Glutamic oxaloacetic transaminase, Median (Q1,Q3)	30 (23, 39.75)	30 (23, 39)	30 (23, 43)	0.572

TBIL, Median (Q1,Q3)	18.33 (12.72, 29.31)	18.17 (13.1, 29.38)	19.3 (11.2, 29.1)	0.972
Direct bilirubin, Median (Q1,Q3)	6.97 (4.74, 13.21)	6.80 (4.84, 11.7)	7.59 (4.2, 14.6)	0.408
Albumin, Median (Q1,Q3)	30.45 (27.56, 34.18)	30.5 (27.47, 34.2)	30.1 (27.76, 34)	0.685
Serum potassium, Median (Q1,Q3)	3.94 (3.62, 4.23)	3.91 (3.59, 4.21)	3.96 (3.68, 4.28)	0.54
Serum sodium, Median (Q1,Q3)	140 (137.4, 142.57)	139.9 (137.5, 141.9)	141.1 (137.2, 143)	0.187
Serum calcium, Median (Q1,Q3)	1.97 (1.87, 2.06)	1.97 (1.88, 2.07)	1.96 (1.87, 2.05)	0.489
Serum creatinine, Median (Q1,Q3)	69 (56, 86)	67 (55, 86)	73 (57, 86)	0.726
Prothrombin time, Median (Q1,Q3)	16.2 (14.7, 17.48)	16.1 (14.7, 17.5)	16.3 (14.7, 17.2)	0.892
Prothrombin time activity, Mean ± SD	67.40 ± 16.37	67.67 ± 16.36	66.79 ± 16.53	0.728
International normalized ratio, Median (Q1,Q3)	1.29 (1.16, 1.43)	1.30 (1.16, 1.45)	1.29 (1.13, 1.4)	0.963
Activated partial thromboplastin time, Median (Q1,Q3)	39.6 (36.73, 43.92)	39.8 (36.9, 43.5)	38.5 (36.6, 44.3)	0.750
Fibrinogen, Median (Q1,Q3)	1.90 (1.5, 2.45)	1.96 (1.51, 2.53)	1.72 (1.47, 2.17)	0.114
Thrombin time, Median (Q1,Q3)	17.8 (16.8, 18.8)	17.8 (16.8, 18.8)	17.7 (16.9, 18.8)	0.962
Blood ammonia, Median (Q1,Q3)	57.5 (40.25, 89)	58.0 (38, 88)	57.0 (46, 89)	0.311
Child score, Median (Q1,Q3)	8 (7, 9)	8 (7, 9)	8 (7, 9)	0.577
Child classification, n (%)				0.702
A	27 (13)	20 (14)	7 (11)	
B	132 (65)	93 (66)	39 (64)	
C	43 (21)	28 (20)	15 (25)	
MADOLHL, Median (Q1,Q3)	7.58 (6.74, 8.24)	7.55 (6.59, 8.28)	7.61 (6.98, 8.12)	0.926
MTDOLHL, Mean ± SD	15.17 ± 3.91	15.16 ± 3.94	15.20 ± 3.87	0.947
MADORHL, Mean ± SD	10.61 ± 2.37	10.72 ± 2.34	10.37 ± 2.43	0.355

MTDORHL, Median (Q1,Q3)	9.57 (8.69, 10.92)	9.92 (8.79, 11.27)	9.16 (8.5, 10.45)	0.032
Maximum distance of hepatic fissure, Median (Q1,Q3)	0.69 (0.49, 0.96)	0.67 (0.46, 0.92)	0.75 (0.52, 1.01)	0.118
Portal vein diameter, Mean ± SD	1.59 ± 0.33	1.58 ± 0.32	1.61 ± 0.36	0.624
Splenic vein diameter, Median (Q1,Q3)	1.02 (0.81, 1.29)	1.03 (0.81, 1.35)	0.97 (0.77, 1.17)	0.196
Cavernous transformation of portal vein, n (%)				0.535
Yes	30 (15)	19 (13)	11 (18)	
No	172 (85)	122 (87)	50 (82)	
Portal vein thrombosis, n (%)				0.006
None	122 (60)	94 (67)	28 (46)	
Thrombus	70 (35)	39 (28)	31 (51)	
Tumor thrombus	10 (5)	8 (6)	2 (3)	
Stent dysfunction, n (%)				0.363
Yes	31 (15)	19 (13)	12 (20)	
No	171 (85)	122 (87)	49 (80)	

Abbreviations: TBIL, Total bilirubin; MADOLHL, Maximum anteroposterior diameter of left hepatic lobe; MTDOLHL, Maximum transverse diameter of left hepatic lobe; MADORHL, Maximum anteroposterior diameter of right hepatic lobe ; MTDORHL, Maximum transverse diameter of right hepatic

Table 2. The multivariate logistic regression analysis of cirrhosis patients undergoing TIPS

	B	SE	OR	CI	Z	*P*
Clinic data						
Cirrhosis etiology	-0.49	0.201	0.613	0.413-0.908	-2.436	0.015
TBIL	-0.037	0.027	0.964	0.914-1.016	-1.354	0.176
Albumin	-0.14	0.058	0.87	0.776-0.974	-2.405	0.016
PT	-0.404	0.167	0.668	0.481-0.926	-2.414	0.016
Blood ammonia	0.009	0.004	1.009	1.001-1.017	2.078	0.038
Radiological data						
Type of shunt channel	-16.572	1824.77	0-Inf	0-Inf	-0.009	0.993
initial stent position	-1.384	0.656	0.25	0.069-0.906	-2.109	0.035
MTDORHL	0.312	0.123	1.366	1.073-1.738	2.534	0.011
PVT	0.769	0.382	2.159	1.021-4.564	2.016	0.044

Abbreviations: TBIL, Total Bilirubin; PT, Prothrombin time; MTDORHL, Maximum Transverse Diameter of the Right Hepatic Lobe; PVT, Portal Vein thrombus

Table 3. The multivariate logistic regression analysis of cirrhosis patients undergoing TIPS（*P*＜0.05）

	B	SE	OR(95% CI)	Z	*P*
Clinic data					
Cirrhosis etiology	-0.49	0.201	0.613(0.413-0.908)	-2.436	0.015
Albumin	-0.14	0.058	0.870(0.776-0.974)	-2.405	0.016
PT	-0.404	0.167	0.668(0.481-0.926)	-2.414	0.016
Blood ammonia	0.009	0.004	1.009(1.001-1.017)	2.078	0.038
Radiological data					
initial stent position	-1.384	0.656	0.250(0.069-0.906)	-2.109	0.035
MTDORHL	0.312	0.123	1.366(1.073-1.738)	2.534	0.011
PVT	0.769	0.382	2.159(1.021-4.564)	2.016	0.044

Abbreviations: PT, Prothrombin Time; MTDORHL, Maximum Transverse Diameter of the Right Hepatic Lobe; PVT, Portal Vein thrombus

Table 4. The comparison of model specificity and sensitivity of different models

Model	Sensitivity	Specificity	Youden	AUC
Training data				
Model C	0.842	0.795	0.637	0.823
Model R	0.579	0.836	0.415	0.790
Model CR	0.737	0.893	0.630	0.901
Validation data				
Model C	0.833	0.714	0.548	0.785
Model R	0.500	0.857	0.357	0.736
Model CR	0.667	0.878	0.544	0.866

Table 5. The comparison of performance of different models

Comparison	Delong test	NRI	P_{NRI}	IDI	P_{IDI}
Training data					
Model C vs Model CR	0.160	0.525	0.027	0.102	0.026
Model C vs Model R	0.326	-0.46	0.054	-0.043	0.457
Model R vs Model CR	0.029	1.199	0	0.145	0
Validation data					
Model C vs Model CR	0.452	0.35	0.270	0.070	0.085
Model C vs Model R	0.314	-0.432	0.172	-0.084	0.096
Model R vs Model CR	0.062	1.095	0	0.154	0.001

Table 6. Hosmer-Lemeshow tests of different Models

Model	Training data		Validation data	
	Statistic	*P*	Statistic	*P*
Model C	3.685	0.298	1.137	0.768
Model R	0.047	0.997	4.183	0.242
Model CR	1.694	0.638	0.815	0.846

Figures

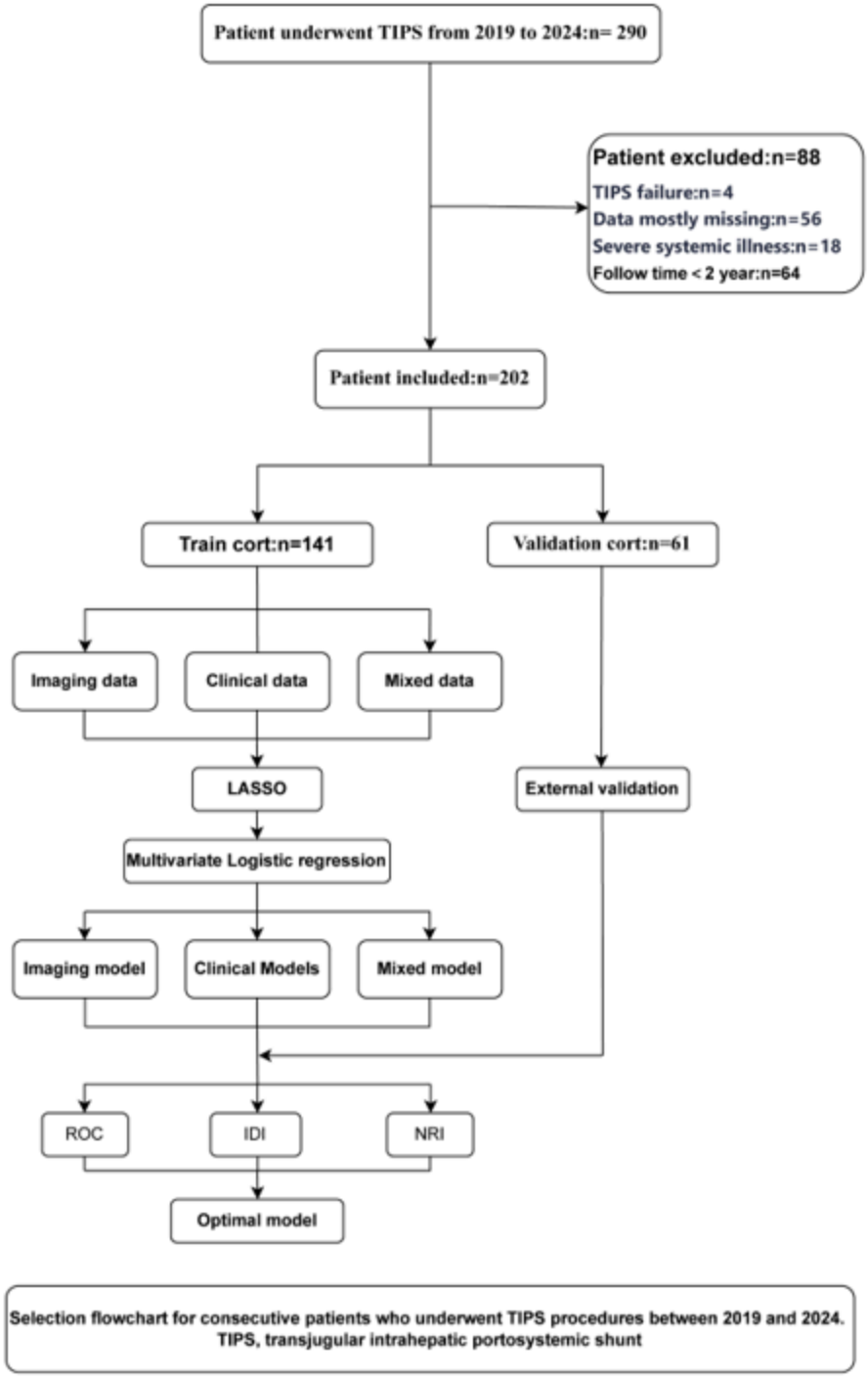

Selection flowchart for consecutive patients who underwent TIPS procedures between 2019 and 2024. TIPS, transjugular intrahepatic portosystemic shunt

Figure 1

Flowchart of the research process

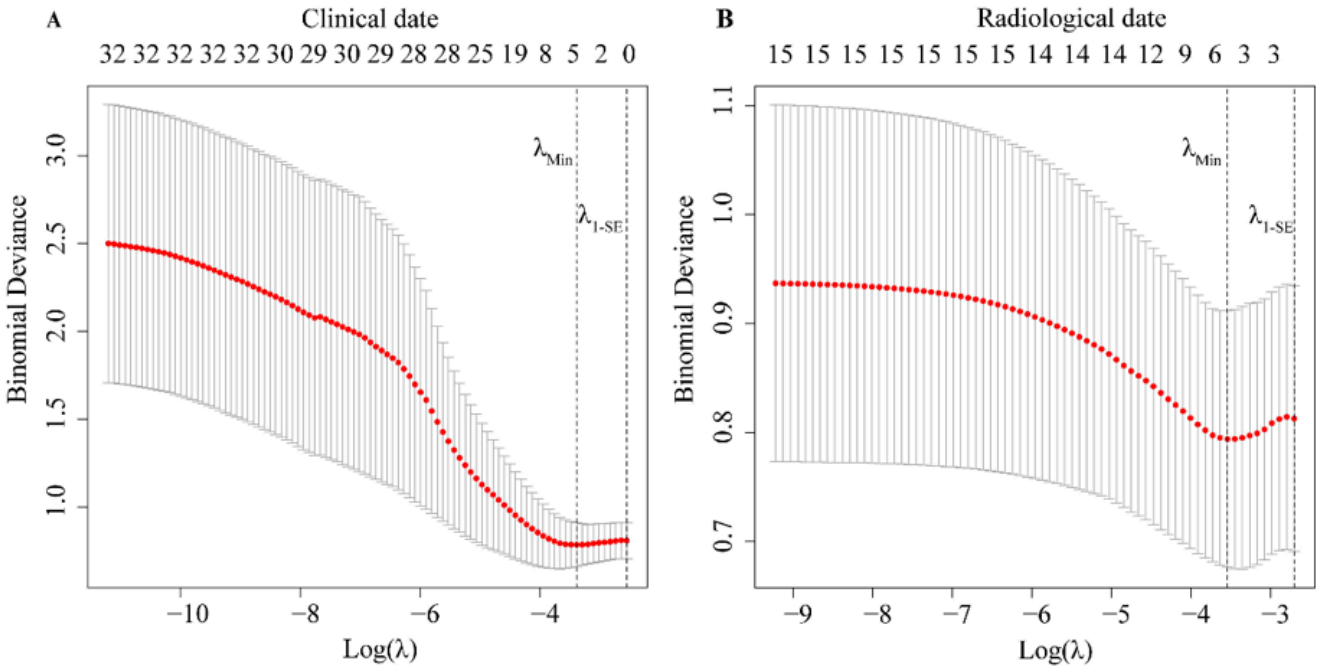

Figure 2

LASSO regression for variable selection

Notes: Figure 2A, LASSO regression analysis of clinical data; Figure 2B, LASSO regression analysis of radiological data. Use LASSO regression analysis to perform feature selection separately on clinical data and radiological data, and select the variables at the λ_{min} value as the selection result. Five variables were ultimately chosen from the clinical data, which are as follows: Cirrhosis etiology, TBIL, Albumin, PT, and Blood ammonia. Four variables were eventually selected from the radiological data, which are as follows: Type of shunt channel, Initial stent position, MTDORHL, PVT. λ_{min} represents the value of λ at the best fit in the LASSO regression selection, and λ_{1SE} represents the value of λ at one standard error to the right of $\lambda_{min.}$ The λ parameter in the LASSO regression analysis of clinical data is: λ_{min}: 0.027, λ_{1SE} 0.100; The λ parameter in the LASSO regression analysis of radiological data is: λ_{min}: 0.021, λ_{1SE} 0.083.

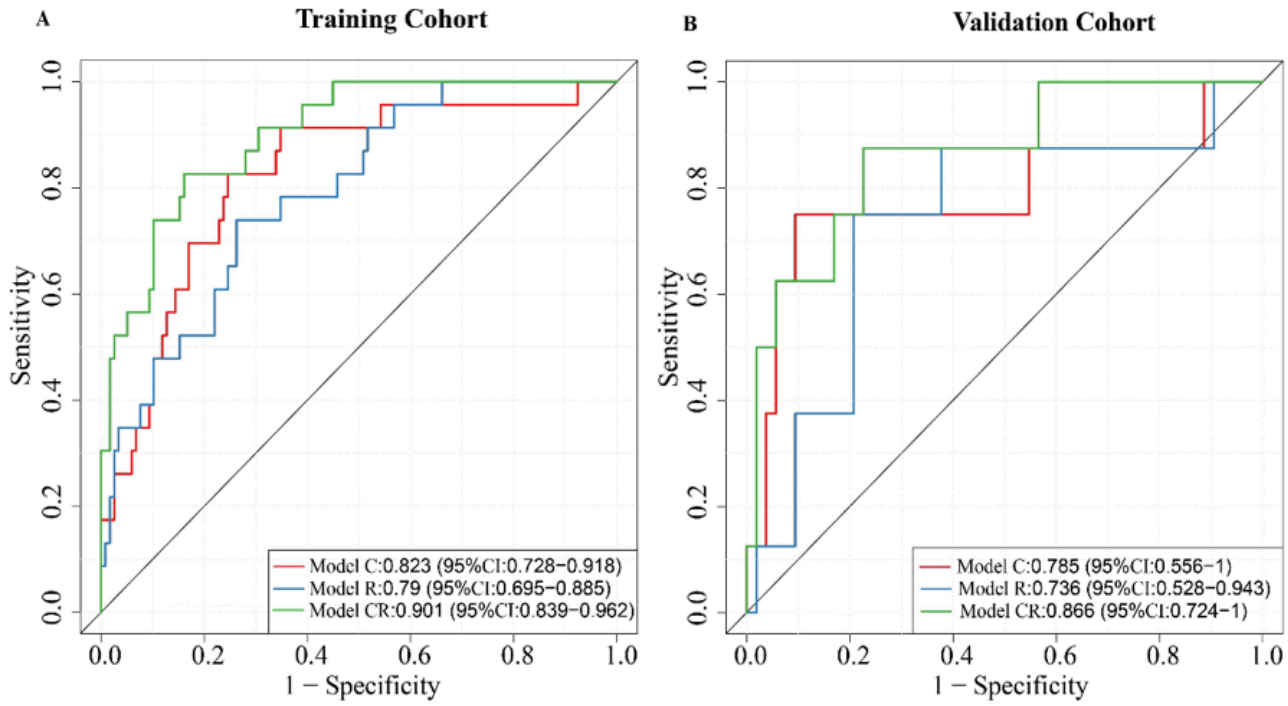

Figure 3

The ROC curves of the three models

Notes: Figure 3A, ROC curve of the training cohort; Figure 3B, ROC curve of the validation cohort.

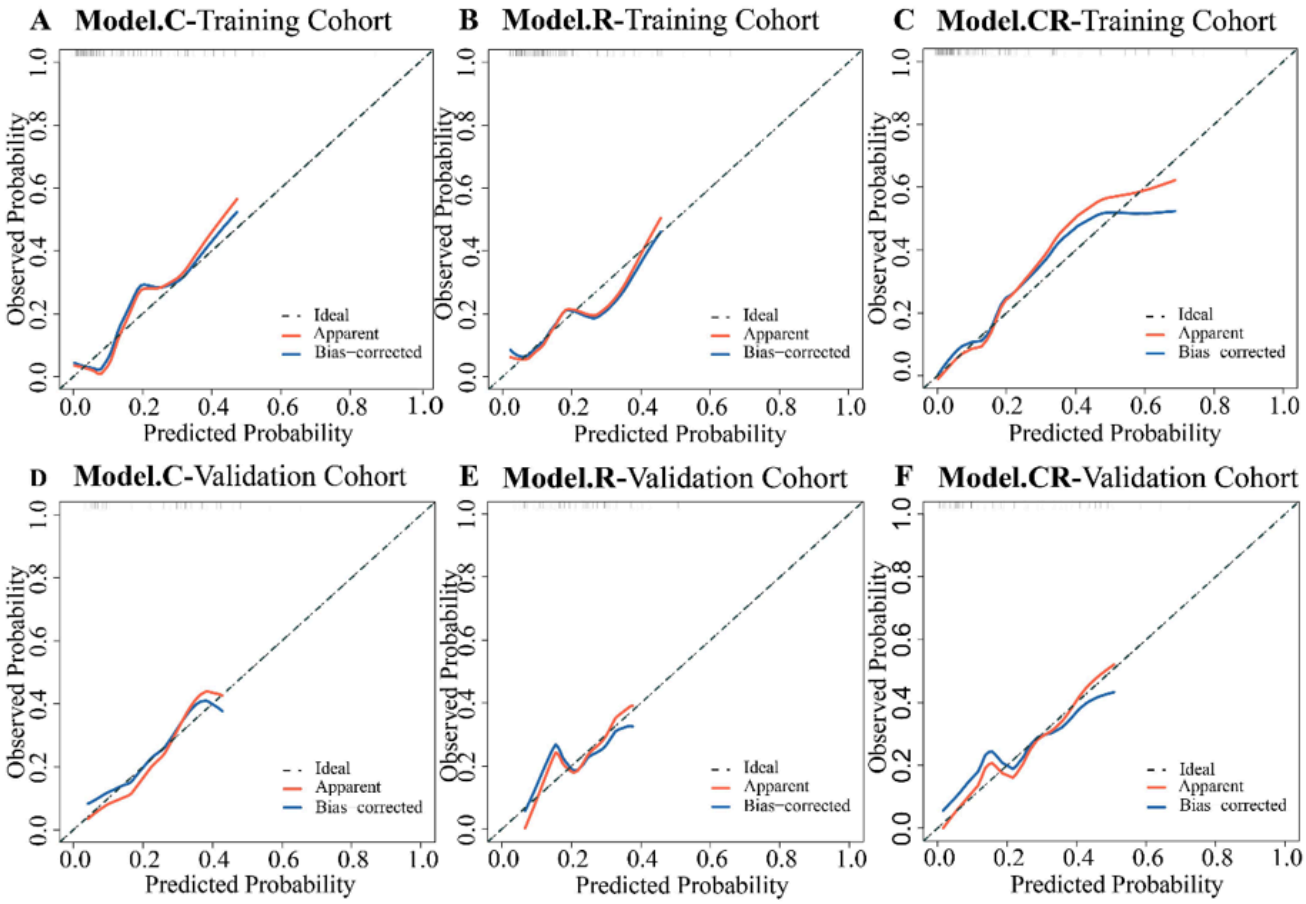

Figure 4

The Calibration curves of three models

Training set: Figure 4A: Calibration curve of Model C; Figure 4B: Calibration curve of Model R；Figure 4C: Calibration curve of Model CR;Validation set: Figure 4D: Calibration curve of Model C; Figure 4E: Calibration curve of Model R；Figure 4F: Calibration curve of Model CR; Model C:Model Clinical;Model R:Model Radiological;Model CR: ModelClinical-Radiological

The dashed line denotes the ideal alignment between predicted and actual outcomes, the blue line represents the model's predicted results, and the red line represents the prediction results after 1000 resamples.

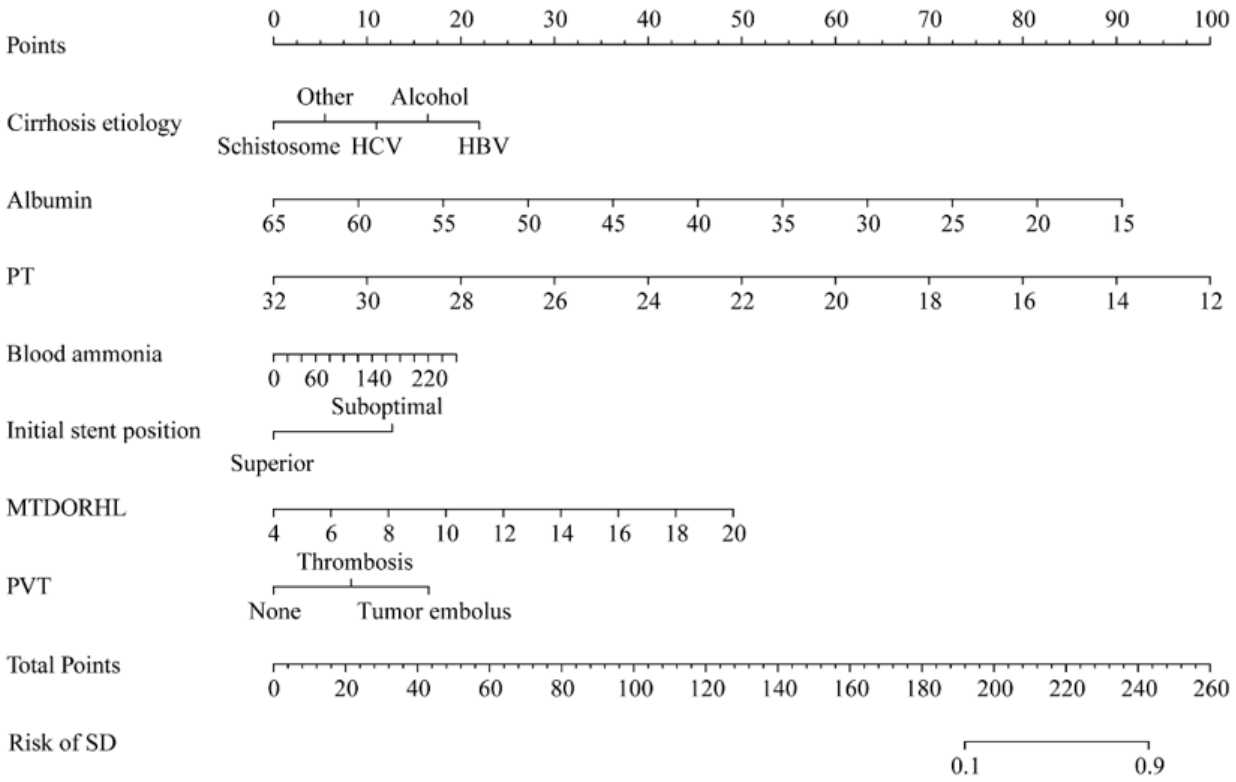

Figure 5

Nomogram development based on the optimal model

Abbreviations: PT, Prothrombin Time; MTDORHL, Maximum Transverse Diameter of the Right Hepatic Lobe; PVT, Portal Vein thrombus

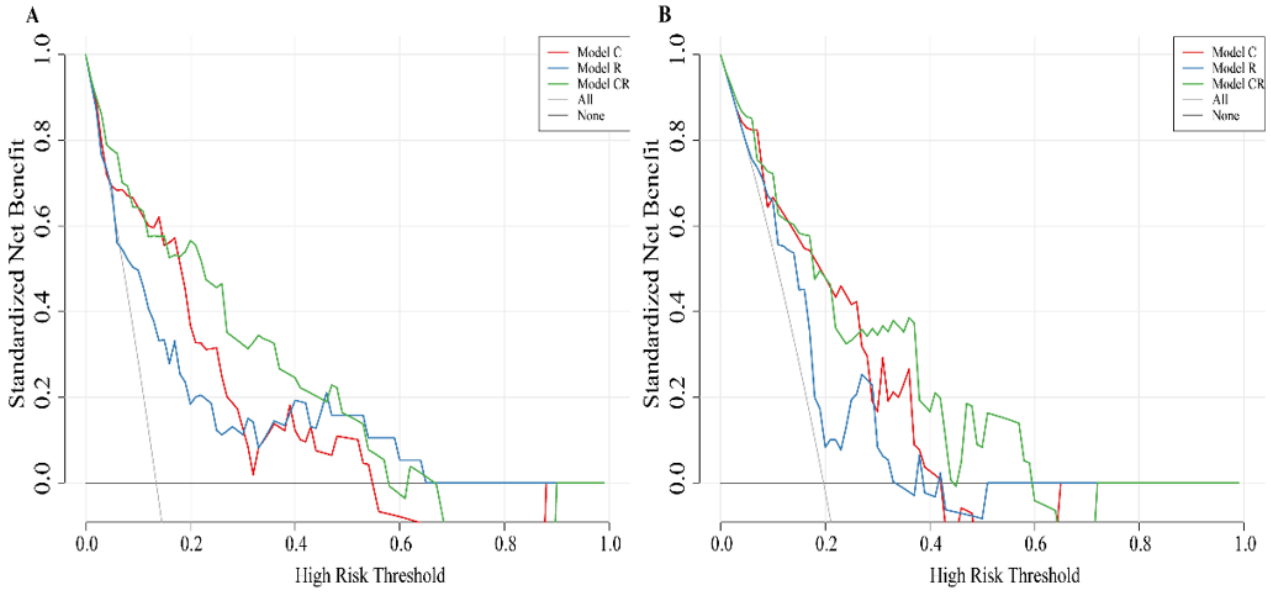

Figure 6

DCA Curves of different Models

Notes: Figure 6A, DCA curve of the training cohort; Figure 6B, DCA curve of the validation cohort.f